*Article*

TRANSPARENT PROCESS

THE EMBO JOURNAL

# The transcription factor Cabut coordinates energy metabolism and the circadian clock in response to sugar sensing

Osnat Bartok[1,†], Mari Teesalu[2,3,†], Reut Ashwall-Fluss[1], Varun Pandey[1], Mor Hanan[1], Bohdana M Rovenko[2,3], Minna Poukkula[3], Essi Havula[2,3], Arieh Moussaieff[4,5], Sadanand Vodala[6], Yaakov Nahmias[4,5], Sebastian Kadener[1,**] & Ville Hietakangas[2,3,*]

## Abstract

**Nutrient sensing pathways adjust metabolism and physiological functions in response to food intake. For example, sugar feeding promotes lipogenesis by activating glycolytic and lipogenic genes through the Mondo/ChREBP-Mlx transcription factor complex. Concomitantly, other metabolic routes are inhibited, but the mechanisms of transcriptional repression upon sugar sensing have remained elusive. Here, we characterize *cabut* (*cbt*), a transcription factor responsible for the repressive branch of the sugar sensing transcriptional network in *Drosophila*. We demonstrate that *cbt* is rapidly induced upon sugar feeding through direct regulation by Mondo-Mlx. We found that CBT represses several metabolic targets in response to sugar feeding, including both isoforms of *phosphoenolpyruvate carboxykinase* (*pepck*). Deregulation of *pepck1* (CG17725) in *mlx* mutants underlies imbalance of glycerol and glucose metabolism as well as developmental lethality. Furthermore, we demonstrate that *cbt* provides a regulatory link between nutrient sensing and the circadian clock. Specifically, we show that a subset of genes regulated by the circadian clock are also targets of CBT. Moreover, perturbation of CBT levels leads to deregulation of the circadian transcriptome and circadian behavioral patterns.**

**Keywords** cabut; circadian; metabolism; nutrient sensing; transcription
**Subject Categories** Metabolism; Transcription
**DOI** 10.15252/embj.201591385 | Received 25 February 2015 | Revised 31 March 2015 | Accepted 1 April 2015 | Published online 27 April 2015
**The EMBO Journal (2015) 34: 1538–1553**

## Introduction

Animals respond to changes in food intake through nutrient sensing pathways that readjust metabolism to maintain homeostasis. Various signaling pathways and transcriptional responses are crucial in the adaptation of an organism to changing dietary conditions (Hietakangas & Cohen, 2009; Havula & Hietakangas, 2012). For example, the paralogous basic helix-loop-helix-leucine zipper (bHLHZ) transcription factors (TFs), carbohydrate-responsive element binding protein (ChREBP), and MondoA coordinate energy metabolism with dietary sugar intake (for review see Havula & Hietakangas, 2012; Filhoulaud *et al*, 2013). These TFs heterodimerize with their common binding partner Mlx to regulate gene expression in response to intracellular glucose-6-phosphate and other phosphorylated hexoses. *Drosophila* encodes single orthologs for ChREBP/MondoA and for Mlx, called Mondo (Mio, CG18362) and Mlx (Bigmax, CG3350), respectively. We have recently shown that loss of functional Mondo-Mlx in *Drosophila* leads to dramatic intolerance for dietary sugars and to impaired glucose and lipid metabolism (Havula *et al*, 2013). In humans, altered ChREBP activity in adipose tissue and liver is associated with severe obesity and polymorphisms of *chrebp* are linked to elevated circulating triglyceride levels (Kooner *et al*, 2008; Benhamed *et al*, 2012; Eissing *et al*, 2013).

Excess dietary sugars are metabolized into lipids, and there is emerging evidence suggesting that high sugar intake, synergistically with genetic risk factors, contributes to obesity and metabolic syndrome (Qi *et al*, 2012; Stanhope *et al*, 2013). Sugar intake activates the ChREBP/Mondo-Mlx-dependent gene expression program to drive fatty acid biosynthesis. This is mediated by binding of ChREBP/Mondo-Mlx to the carbohydrate response elements (ChoREs) in the promoters of lipogenic genes including *fatty acid*

1 Biological Chemistry Department, Silberman Institute of Life Sciences, The Hebrew University of Jerusalem, Jerusalem,Israel
2 Department of Biosciences, University of Helsinki, Helsinki, Finland
3 Institute of Biotechnology, University of Helsinki, Helsinki, Finland
4 Department of Cell Biology, Silberman Institute of Life Sciences, The Hebrew University of Jerusalem, Jerusalem, Israel
5 Center for Bioengineering, The Hebrew University of Jerusalem, Jerusalem, Israel
6 Howard Hughes Medical Institute, Brandeis University, Waltham, MA, USA
*Corresponding author. Tel.: +358 2 94158001; E-mail: ville.hietakangas@helsinki.fi
**Corresponding author. Tel.: +972 2 6585099; E-mail: skadener@mail.huji.ac.il
†These authors contributed equally to this work

*synthase* (*Fas*) and *acetyl-CoA carboxylase* (*ACC*) (Ishii *et al*, 2004). Flies lacking functional Mondo-Mlx display elevated circulating glucose, trehalose and reduced adiposity, but the metabolic effector genes underlying these phenotypes are incompletely understood (Sassu *et al*, 2012; Havula *et al*, 2013).

In addition to fatty acids, biosynthesis of triglycerides requires glycerol-3-phosphate. Glycerol-3-phosphate is synthesized by three alternative pathways: glycolysis, phosphorylation of diet-derived glycerol by glycerol kinase, and from TCA cycle intermediates via the so-called glyceroneogenesis pathway (Ballard *et al*, 1967; Hanson & Reshef, 2003; Jin *et al*, 2013). A rate-limiting reaction in the glyceroneogenesis pathway is catalyzed by phosphoenolpyruvate carboxykinase (PEPCK) (Hanson & Reshef, 2003). PEPCK controls the cataplerotic flux, which converts the oxaloacetate (OAA) from the TCA cycle into phosphoenolpyruvate (PEP). PEP can be further routed into glucose (trehalose in insects (Becker *et al*, 1996)) through gluconeogenesis or glycerol-3-phosphate through glyceroneogenesis. PEPCK is present as a cytoplasmic and a mitochondrial isoform, both of which have shown to contribute to gluconeogenesis (Stark *et al*, 2014). As *pepck* plays a key role in adjusting the direction of flux of central carbon metabolism, it is under tight nutritional control. It is well established in mammals that the hormonal insulin/glucagon axis controls *pepck* expression via transcription factors CREB and FoxO1, both of which are active during starvation (high glucagon, low insulin) (Oh *et al*, 2013). However, whether cell-intrinsic nutrient sensing mechanisms contribute to PEPCK regulation has remained poorly understood.

Circadian clocks time most physiological and behavioral processes to 24-h rhythms (Hardin, 2011; Partch *et al*, 2014). Among these processes is metabolism, which is strongly controlled by the circadian system (Bass, 2012; Peek *et al*, 2012; Masri & Sassone-Corsi, 2014; Dibner & Schibler, 2015). In *Drosophila,* this control manifests mainly at the transcriptional level (Xu *et al*, 2008, 2011). Metabolism feeds back to the circadian system, as dietary cues (i.e., restriction feeding) and metabolites have profound impact on the circadian system (Mattson *et al*, 2014). Circadian clocks are spread throughout the body and are present in most cells. Circadian clocks work cell autonomously, although cell-to-cell communication is known to provide robustness to circadian behavior (Weiss *et al*, 2014). In *Drosophila,* circadian control of metabolism is achieved mainly in the fat body and it is involved in the timed expression of hundreds of metabolic genes, including the ones involved in sugar and fat metabolism (Xu *et al*, 2008, 2011). The importance of this regulation is highlighted by the fact that disruption of circadian rhythms either by genetic or environmental cause is strongly associated with metabolic imbalances, diabetes, and obesity (Bass, 2012; Peek *et al*, 2012).

Transcription factors (TFs) form hierarchical regulatory networks, which allow the integration of different input signals and the generation of complex and robust biological responses. In the context of sugar sensing, our previous work demonstrated that ChREBP/MondoA-Mlx strongly regulates the TF *cabut* (*cbt*) in *Drosophila*, which is involved in sugar tolerance by a yet unknown mechanism (Havula *et al*, 2013). The closest mammalian homologs of CBT are Krüppel-like factors Klf10 and Klf11 (Subramaniam *et al*, 2010; Spittau & Krieglstein, 2012). *klf10* expression is promoted by sugar in a ChREBP-dependent manner (Iizuka *et al*, 2011), whereas *klf11* expression is elevated upon starvation (Zhang *et al*, 2013), suggesting that *klf10* is the functional ortholog of *cbt* in the context of sugar sensing transcriptional network. Interestingly, the circadian clock can regulate *klf10* levels, and hence, this transcription factor might act as a link between the circadian and metabolic systems (Guillaumond *et al*, 2010). Furthermore, a variant of the *klf10* gene is proposed to contribute to the risk of type-2 diabetes (Gutierrez-Aguilar *et al*, 2007).

Here, we found that CBT is a central mediator of a repressive branch of the intracellular sugar sensing transcriptional network in *Drosophila*. We demonstrate that *cbt* expression is activated upon sugar feeding through direct regulation by the sugar sensing TF complex Mondo-Mlx. Genome-wide analyses reveal that CBT contributes to rapid and persistent repression of metabolic genes upon sugar feeding. CBT directly represses both *pepck* isoforms, inhibiting cataplerosis during sugar feeding. Failure in this regulatory axis leads to loss of glucose and glycerol homeostasis and to lethality observed in animals lacking functional Mondo-Mlx. Last but not least, we found that CBT integrates feeding information into a subset of metabolic genes, which are regulated by the circadian clock. In sum, here we identify and characterize a transcriptional circuit that allows animals to readjust their central carbon metabolism as well as circadian clock with respect to sugar feeding.

## Results

### *cbt* is regulated by dietary sugar through Mondo-Mlx

Based on our earlier findings on *cbt* being essential for sugar tolerance (Havula *et al*, 2013), we decided to explore how *cbt* is regulated upon sugar feeding. To this end, we measured *cbt* levels at different times after re-feeding with 5 or 10% sucrose. Indeed, we observed a twofold increase in *cbt* levels 6 h following sugar re-feeding in adults (Supplementary Fig S1A). In contrast, re-feeding with protein did not lead to increased *cbt* expression, but rather to a small decrease (Supplementary Fig S1B). Given our previous findings, we hypothesized that the sugar-induced expression of *cbt* might be mediated by Mondo-Mlx activity. As *mlx* null mutants ($mlx^1$) are pupal lethal (Havula *et al*, 2013), we sought to explore *cabut* expression in the larvae. Indeed, *cbt* expression was upregulated in larvae that had been transferred to high sugar/high protein diet (10% yeast, 20% sucrose) compared to ones remaining in low sugar/high protein diet (10% yeast), and this upregulation was fully abrogated in $mlx^1$ mutants (Fig 1A). These results suggest that the Mondo-Mlx dimer may directly regulate *cbt* expression. Supporting this possibility, we found two conserved consensus motifs for putative binding of this heterodimer, the carbohydrate-responsive elements (ChoRE), near the *cbt* transcription start site (TSS): one was located about one kilobase upstream and the other a few hundred bases downstream the annotated TSS (Fig 1B and C). We performed chromatin immunoprecipitation (ChIP) from *Drosophila* S2C cells using anti-Mlx antibodies or preimmune serum as a negative control. Indeed, Mlx strongly bound these two putative ChoREs in the *cbt* promoter region (Fig 1D). Moreover, we observed that Mlx binding to *cbt* promoter was significantly

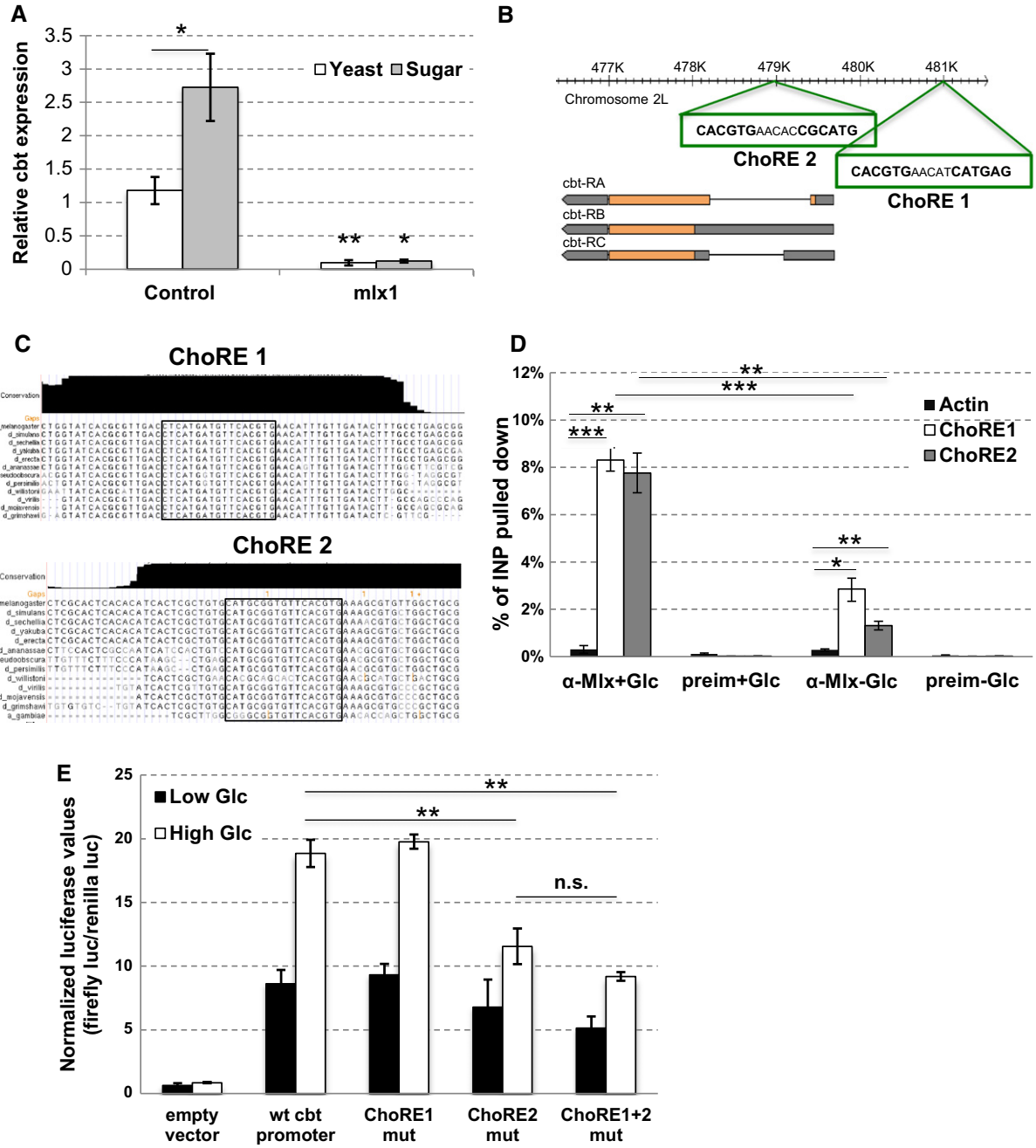


**Figure 1. *cbt* is a direct target of Mondo-Mlx-mediated sugar sensing.**

A *cbt* expression is sugar inducible and Mlx dependent. *cbt* mRNA levels in control (precise excision of P-element line) and *mlx*$^{1}$ mutant 2$^{nd}$ instar larvae after 8 h of 10% yeast (Yeast) or 10% yeast and 20% sucrose feeding (Sugar). *Actin* was used as a reference gene. Error bars indicate SD, $n = 3$. *$P < 0.05$; **$P < 0.01$.

B Two putative ChoRE sites in the *cbt* gene region.

C Conservation of the putative ChoRE sites in the *cbt* gene region in *Drosophila* species.

D ChIP from S2C cells with anti-Mlx antibody or pre-immune serum in the presence or absence of 50 mM glucose (6 h). The percentage of input pulled down was determined by qPCR. *Actin* was used as a negative control. Error bars indicate SD, $n = 3$. *$P < 0.05$, **$P < 0.01$, ***$P < 0.001$.

E ChoRE2 is required for full *cbt* promoter activity and sugar responsiveness. Luciferase reporter assay with *cbt* promoter in HepG2 cells grown in low (5.5 mM) or high (25 mM) glucose. Error bars indicate SD, $n = 3$. **$P < 0.01$.

increased in high glucose media (Fig 1D, compare ± Glc). To functionally test the importance of the ChoREs, we constructed a luciferase reporter containing −1,961 to +641 region of the *cbt* promoter. We also generated versions of this promoter in which the putative ChoREs were mutated. As the reporter failed to display glucose responsiveness in S2C cells (data not shown), we performed the experiments in human HepG2 hepatocellular carcinoma cells, which are a well-established model system for

 

ChREBP-mediated gene regulation (Jeong *et al*, 2011). Indeed, the *cbt* promoter was activated by glucose stimulation, and the reporter activity was significantly inhibited when ChoRE2 was mutated (Fig 1E). In conclusion, our experiments show that *cbt* is induced by dietary sugars likely through direct binding of Mondo-Mlx to the ChoREs in the *cbt* promoter.

### *cbt* regulates the expression of genes involved in metabolism

CBT is known to repress its own expression (Belacortu *et al*, 2012), but beyond that, the transcriptional targets and function of CBT are still poorly understood. Therefore, we sought to identify CBT-regulated transcriptome in adult *Drosophila*. We utilized the GAL4-UAS system to generate flies in which *cbt* is down- or upregulated. We tested several GAL4-UAS drivers in combination with UAS-*cbt* or UAS-*cbt* RNAi. Most of these combinations resulted in high or total developmental lethality. We were able to obtain adult flies by using a GAL4 driver that expresses the gene of interest only in cells harboring an active circadian clock (*tim-gal4* driver). The *tim-gal4* driver expresses in approximately half of the cells of the fly head, including the brain, eyes, and the fat body, the fly equivalent of the mammalian liver and adipose tissue (Xu *et al*, 2008). To overexpress *cbt*, we utilized the *tim-gal4* driver line in combination with a UAS-*cbt*FLAG transgene (Muñoz-Descalzo *et al*, 2005); these flies will be referred to as cbtOE flies. To downregulate *cbt,* we used the same driver in combination with a publicly available *cbt* RNAi transgene (NIG.4427R from NIG-Fly Stock Center), a UAS-dcr2 transgene, and a mutant *cbt* allele ($cbt^{E1}$ (Muñoz-Descalzo *et al*, 2005)) in heterozygosis. We will call these cbtRNAi flies. After verifying the levels of CBT by Western blot (Supplementary Fig S2A), we assessed the transcriptomes in heads of control, cbtRNAi, and cbtOE flies using oligonucleotide microarrays. More than 1,000 genes were significantly affected by at least one of the manipulations in *cbt* levels (Fig 2A, Supplementary Dataset S1). Among them, genes related to neuronal function, immunity, and metabolism were specifically enriched (Fig 2B; Supplementary Fig S2B). In particular, we found that genes involved in carbohydrate metabolism were strongly affected by *cbt* up- or downregulation (Fig 2B and Supplementary Fig S3). Previously, a role of CBT in regulating circadian transcription was suggested by the fact that the circadian transcriptional activator CLK binds CBT promoter in a timely fashion (Abruzzi *et al*, 2011). Interestingly, we found a significant number of CLK-controlled genes among the genes downregulated by CBT ($P < 0.0001$), suggesting that in addition to metabolic gene expression *cbt* might regulate the circadian transcriptome (Abruzzi *et al*, 2011).

### CBT constitutes a repressive branch of the sugar sensing transcriptional network

As *cbt* expression is induced by sugar intake, we decided to determine the role of CBT in the sugar-induced transcriptional response. To do so, we profiled the transcriptomes using 3′ RNA-seq of control and cbtRNAi flies after they had been starved and exposed to different levels of sucrose for 18 h (see scheme in Supplementary Fig S4A). After a very conservative analysis of the data, we found that levels of 72 transcripts were strongly affected by sugar intake at this time point. Most of these mRNAs (51) displayed decreased expression in response to this dietary manipulation (Supplementary Dataset S2). Of these 51 genes, 22 mRNAs were downregulated in a CBT-dependent manner (Fig 2C; Supplementary Dataset S2; Supplementary Fig S4B). In addition, we found eight more CBT-regulated mRNAs by looking at genes that are significantly more affected by sugar intake in cbtRNAi flies compared with control flies (Supplementary Dataset S3). Among the CBT-repressed targets, we found transcripts encoding proteins with function in lipolysis, gluconeogenesis, and glycerol metabolism including *brummer* (*bmm*) lipase, *fructose-1,6-bisphosphatase* (*fbp*), *phosphoenolpyruvate carboxykinase* (*pepck*), and *glycerol kinase* (*Gyk*) (Supplementary Fig S4B). Notably, the *pepck, fbp*, and *Gyk* encode proteins with related functions. PEPCK participates with FBP in gluconeogenesis, and Gyk and PEPCK control biosynthesis of glycerol-3-phosphate, albeit through two distinct pathways. These results demonstrate that CBT has a central role in repressing the expression of key metabolic genes in response to dietary sugars.

In order to temporally characterize the transcriptional response to dietary sugars with respect to CBT function, we performed a transcriptomic analysis of adult fly heads harvested at different times following sugar intake after starvation. Our analysis identified 520 mRNAs that changed levels significantly at least at one of the time points (Fig 2D; Supplementary Dataset S4). Clustering analysis allowed us to identify ten transcriptional modules with different temporal patterns of expression following sugar intake (Fig 2D and E

**Figure 2. CBT represses metabolic genes upon sugar feeding.**

A Heatmap representing the microarray data obtained from control, cbtRNAi, and cbtOE flies. From each strain, fly heads at two different time points during the day–night cycle (3 h after light on or light off) were collected. Based on statistical analysis, levels of 1,023 mRNAs were affected in one or more of the strains (FDR < 0.2 and fold change > 1.5).

B Histogram showing the fold change of the top 20 genes with expression altered by downregulation (top panel) or upregulation (bottom panel) of CBT. For each gene, the fold change was calculated as the ratio between the values obtained in cbtOE and cbtRNAi flies.

C Heatmap representing the 3′ RNA-seq data of control and cbtRNAi adult flies following 24 h of sugar refeeding (left). For clarity, selected transcripts are displayed. mRNAs were classified into three main groups depending on their response to sugar: genes that are downregulated similarly in control and cbtRNAi flies, genes that are not significantly affected in control but upregulated in cbtRNAi flies, and genes that are downregulated in control flies but are not differentially expressed following sugar intake in cbtRNAi flies. The regulation by sugar and CBT is represented on the right.

D Heatmap representing 3′ RNA-seq data of genes that change significantly following sugar intake. The transcriptome assay was performed from heads of adult flies that had been starved for 16 h and transferred to vials containing food with 5% sucrose. The arrow indicates the time when the flies were re-fed. The levels of 520 mRNAs were significantly changed at least in one of the time points.

E Two transcriptional modules that contain mRNAs that were strongly downregulated following sugar intake. The graphs were obtained by averaging normalized expression of all the genes in these modules. CBT targets are clustered into the module displaying rapid and persistent downregulation by sugar.

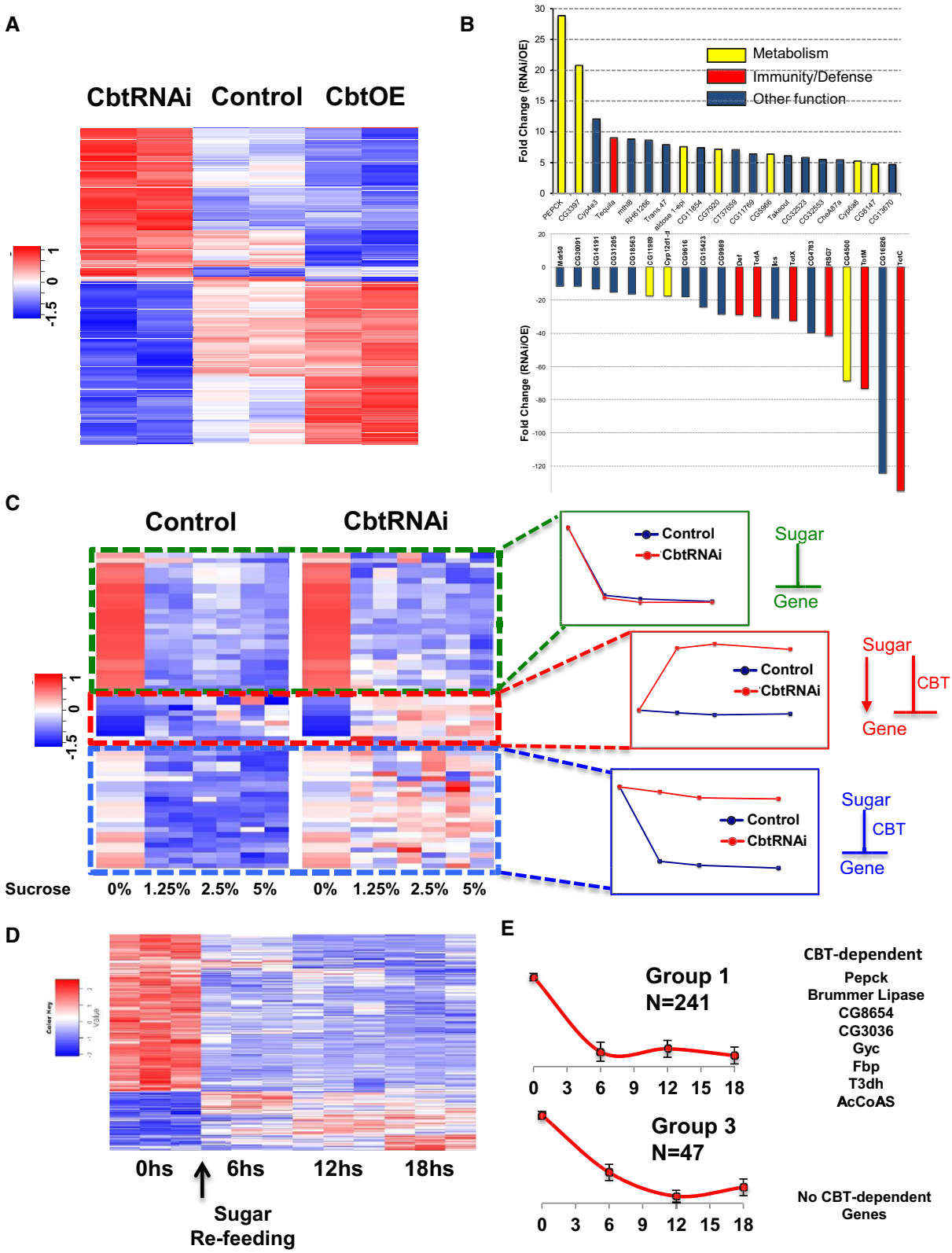


Figure 2.

and Supplementary Fig S5; Supplementary Dataset S5; see Materials and Methods for details). Interestingly, the majority of CBT-dependent targets clustered into Group 1 containing genes that are repressed by sugar feeding in a rapid and persistent manner (Fig 2E). This further supports the conclusion that CBT is a sugar-activated transcriptional repressor.

### *pepck* isoforms are negatively regulated by the Mondo-Mlx/CBT network

One of the strongest CBT-regulated genes across all our genomic analyses was *pepck* (CG17725) (Fig 2B and Supplementary Fig S4B). In mammals, PEPCK exists as cytoplasmic (PEPCK-C) and mitochondrial (PEPCK-M) isoforms, displaying partially redundant functions (Stark *et al*, 2014). *Drosophila* genome also encodes two genes homologous to mammalian PEPCK isoforms, namely CG17725 (called as *Pepck* in FlyBase) and the neighboring gene CG10924. CG17725 lacks an identifiable mitochondrial targeting sequence, while MitoProt II predicts that CG10924 is likely targeted to mitochondria (likelihood 0.82). We call the CG17725 and CG10924 as *pepck1* and *pepck2*, respectively. In adult flies, *cbt* overexpression resulted in strong downregulation of *pepck1* expression, whereas cbtRNAi flies displayed elevated *pepck1* mRNA levels (Fig 3A). Moreover, sugar feeding rapidly and persistently downregulated the expression of *pepck1*, and this downregulation was prevented by RNAi-mediated depletion of CBT (Fig 3B and Supplementary Figs S5 and S6A). Feeding with protein caused only a modest downregulation of *pepck1* expression (Supplementary Fig S6B). Similar to adults, sugar feeding led to downregulation of *pepck1* expression in larvae (Supplementary Fig S6C). In fed larvae, two independent RNAi lines against CBT caused upregulation of *pepck1* expression (Fig 3C; Supplementary Fig S6D), providing further evidence for CBT-mediated repression of *pepck1*. Consistent with the finding that CBT function is dependent on functional Mondo-Mlx, *pepck1* expression was also strongly elevated in *mlx* mutant larvae (Fig 3C). Moreover, fat body-specific overexpression of CBT in the *mlx* mutant background was sufficient to downregulate *pepck1* expression (Fig 3D), consistent with the model that CBT acts downstream of Mondo-Mlx to repress *pepck1*. CBT knockdown and loss of *mlx* led to comparable upregulation of *pepck2* (Fig 3E). Moreover, fat body-specific overexpression of CBT in the *mlx* mutant also rescued *pepck2* expression levels (Supplementary Fig S6E). In conclusion, our data demonstrate that CBT represses both *Drosophila pepck* isoforms.

As CBT has been shown to possess transcriptional repressor activity (Belacortu *et al*, 2012), we speculated that CBT might directly repress the transcription of the *pepck* genes. To test this possibility, we performed ChIP from fly heads using an anti-CBT antibody followed by quantitative PCR. As CBT is known to act as an autoregulator (Belacortu *et al*, 2012), we used *cbt* promoter as a positive control. We found that CBT strongly binds to a region between the two *pepck* genes (Fig 3F and G), providing evidence that the expression of *pepck* isoforms is directly repressed by CBT. Krüppel-like TFs bind to GC-rich areas (Brown *et al*, 2005; Belacortu *et al*, 2012), and indeed, the region enriched for CBT binding possesses three GC-rich segments (Fig 3G).

### *pepck1* is dispensable for viability and growth but essential for glycerol and glucose homeostasis

To address the physiological role of PEPCK1 in *Drosophila*, we generated a *pepck1* deletion mutant by imprecise P-element (EY10042) excision (*pepckΔ84;* Fig 4A). The deletion removed 108 amino acids from the conserved PEPCK1 N-terminus (34.5% identical to this region of human PEPCK-C). Quantitative RT–PCR revealed that the deletion strongly reduced *pepck1* mRNA levels (Fig 4B). Thus, the deletion mutant is a null or a strong hypomorphic allele of *pepck1*. To reduce possible compensatory effects by *pepck2*, we used the *pepckΔ84* allele in *trans* with a deficiency uncovering both *pepck* loci (*Df(2R)ED3636*). Surprisingly, we found that the *pepckΔ84/Df(2R)ED3636* mutants were fully viable (Fig 4C). Careful phenotypic characterization of the *pepckΔ84/Df(2R)ED3636* mutants revealed modest, but significant reduction of feeding in the *pepck1*-deficient animals (Supplementary Fig S7A). However, we did not observe a delay of development or reduced pupal volume, which are typical phenotypes of starved animals (Supplementary Fig S7B and C).

Next, we wanted to analyze whether *pepck1*-deficient animals displayed alterations of metabolite profile. Levels of circulating glucose and trehalose were moderately, but significantly downregulated in the *pepck1*-deficient animals (Fig 4D and E). Trehalose is the most abundant circulating sugar in insects and the product of fat body gluconeogenesis and glycogenolysis (Becker *et al*, 1996). In addition to the moderate effects on glucose metabolites, steady state levels of circulating glycerol were strongly downregulated in *pepckΔ84/Df(2R)ED3636* larvae as well as in *pepckΔ84* homozygotes (Fig 4F). RNAi against either of the *pepck* isoforms also led to reduced circulating glycerol levels (Supplementary Fig S7D), suggesting that the *pepck* isoforms have overlapping functions, but are not fully functionally redundant. Moreover, triglyceride levels were significantly reduced in the *pepck1* mutant flies (Fig 4G). In contrast to the glucose and glycerol metabolites, levels of glutamate and glutamine remained unchanged (Supplementary Fig S7E), demonstrating that the loss of *pepck1* leads to a specific metabolic imbalance. Metabolites, which are downstream of PEPCK-mediated cataplerosis, are present at lower levels in *pepck1* mutants. In conclusion, our data reveal a prominent role for *pepck1* in glycerol and triglyceride homeostasis and a moderate effect on steady state glucose and trehalose levels. However, the metabolic changes in the *pepck1*-deficient animals have no impact on growth or survival of the larvae.

### The Mondo-Mlx/CBT network inhibits PEPCK-mediated cataplerosis

Next, we addressed the physiological consequences of the PEPCK regulation by the Mondo-Mlx/CBT network. As PEPCK catalyzes the conversion of oxaloacetate (OAA) to phosphoenolpyruvate (PEP), we started by measuring the ratio of these metabolites. Interestingly, we observed that *cbt* knockdown as well as loss of *mlx* led to a significant elevation of the PEP/OAA ratio (Fig 5A and B), consistent with the elevated *pepck* expression in these genotypes. As *pepck1* mutants displayed reduced level of circulating glycerol, we analyzed glycerol levels upon inhibition of the Mondo-Mlx/CBT network. While cbtRNAi showed no dramatic changes in glycerol homeostasis (data not shown), $mlx^1$ mutants displayed strongly elevated circulating glycerol levels. Similar results were obtained by mondoRNAi (Supplementary Fig S8A). Moreover, we could rescue this phenotype by fat body-specific expression of Mlx (Fig 5C). To directly test whether this phenotype is due to deregulated PEPCK activity, we analyzed the phenotypes of $mlx^1$; *pepckΔ84/Df(2R)ED3636* double mutants. Indeed, the high circulating glycerol levels of *mlx* mutants were rescued

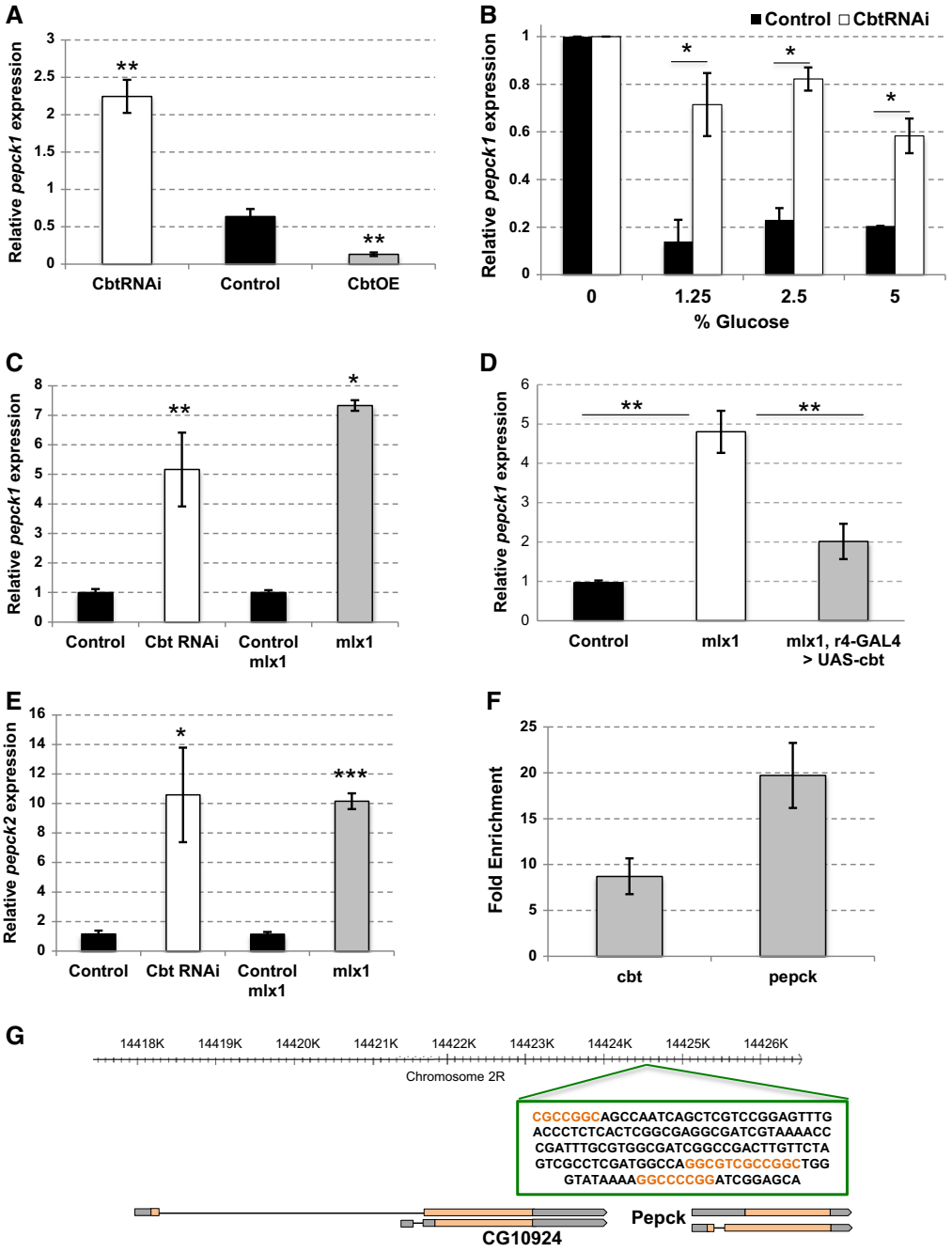


**Figure 3. The Mondo-Mlx/CBT network negatively regulates the expression of *pepck* isoforms.**

A *pepck1* mRNA levels in heads of cbtRNAi, control (*yw*; UAS-cbt), and cbtOE adult flies. *pepck1* levels were normalized to *rp49*. Error bars indicate SD, $n = 6$. $^{**}P < 0.01$.

B *pepck1* mRNA levels in the heads of control (+/cbt$^{E1}$-UAS-*cbt* RNAi) or cbtRNAi adult flies that were starved for 16 h and then exposed to food containing different concentrations of sucrose for 18 h. RNA-seq data. Error bars indicate SD, $n = 3$. $^{*}P < 0.05$.

C *pepck1* mRNA levels in 1$^{st}$ instar *cbt* knock-down and *mlx1* mutant larvae. *Actin* was used as a reference gene. Control (Tub-GAL80$^{ts}$; Tub-GAL4 > ), cbtRNAi (Tub-GAL80$^{ts}$; Tub-GAL4 > cbtRNAi NIG 4427R-1), control for *mlx*$^{1}$, and *mlx*$^{1}$ mutants were grown on 20% yeast. Error bars indicate SD, $n = 3$. $^{*}P < 0.05$, $^{**}P < 0.01$.

D *pepck1* mRNA levels in 1$^{st}$ instar control (precise excision of P-element line) larvae, *mlx*$^{1}$ mutants, and in *mlx*$^{1}$ mutants with fat body-specific over-expression of *cbt* (*mlx*$^{1}$, r4-GAL4 > UAS-cbt). *Actin* was used as a reference gene. Error bars indicate SD, $n = 3$ (control and *mlx*$^{1}$) and $n = 7$ (*mlx*$^{1}$; r4-GAL4 > UAS-cbt). $^{**}P < 0.01$.

E *pepck2* mRNA levels in 1$^{st}$ instar *cbt* knock-down and *mlx*$^{1}$ mutant larvae. *Actin* was used as a reference gene. Control (Tub-GAL80$^{ts}$; Tub-GAL4 > ), cbtRNAi (Tub-GAL80$^{ts}$; Tub-GAL4 > cbtRNAi NIG 4427R-1), control and *mlx*$^{1}$ mutants were grown on 20% yeast. Error bars indicate SD, $n = 3$. $^{*}P < 0.05$, $^{***}P < 0.001$.

F Fold enrichment of ChIP-PCR in the promoter regions of *cbt* and *pepck1* performed from adult heads. The fold enrichment was obtained by normalization of signals in the immunoprecipitates to those in input fractions. Normalization was performed using primer pairs that amplify non-specific DNA regions. Error bars indicate SD, $n = 3$.

G Schematic representation of the CBT binding sites in between the PEPCK-encoding genes. GC-rich regions are highlighted.

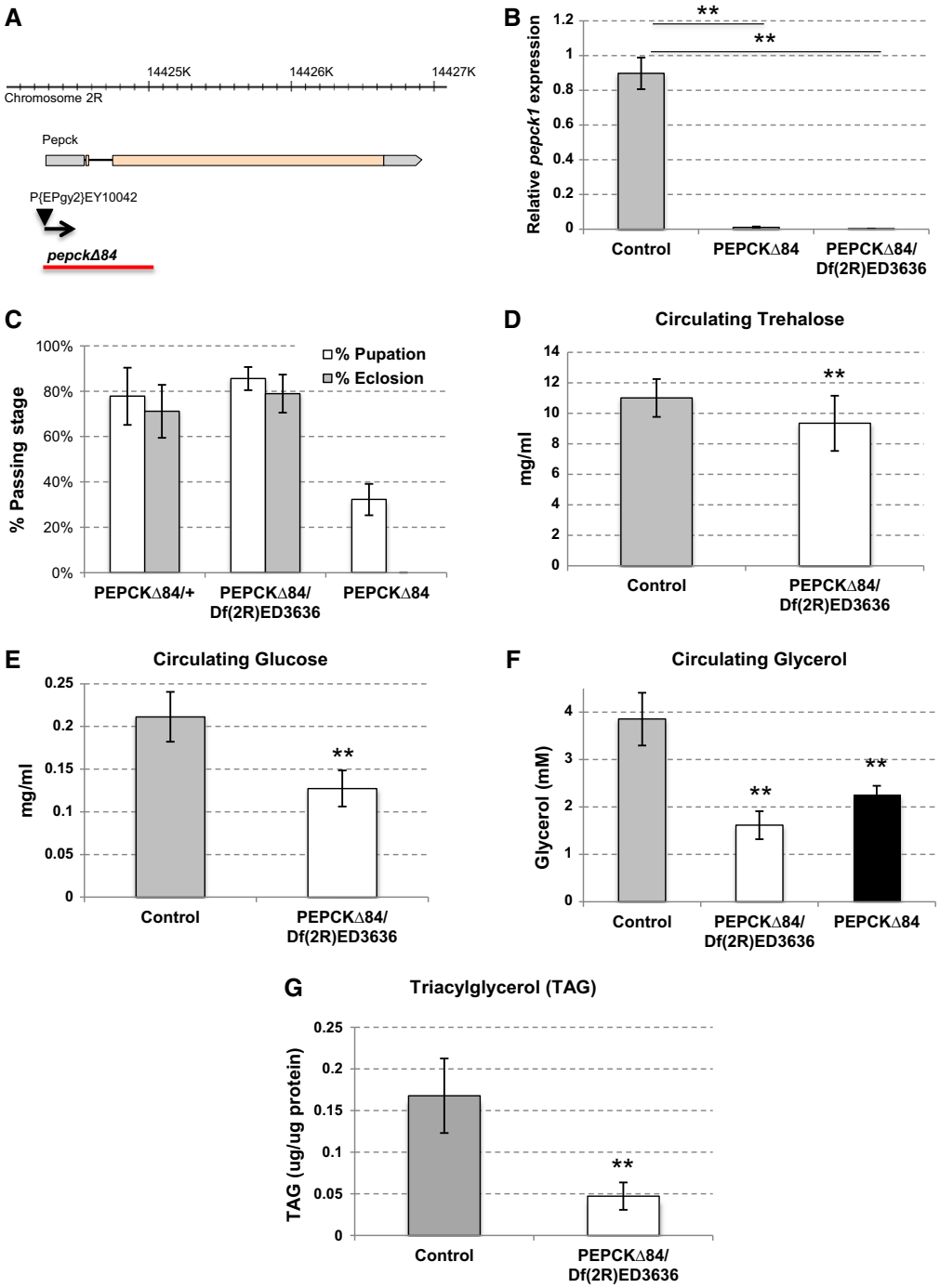


**Figure 4. *pepck1* mutants are viable but display strongly reduced free glycerol and triglyceride levels.**

A Schematic representation of the *pepckΔ84* allele generated by imprecise P-element excision. The resulting deletion spans 825 base pairs and removes the transcription start site, start codon, and sequence encoding 108 amino acids of the N-terminal region of the protein.

B qPCR analysis of *pepck1* expression levels in control (precise excision of P-element line crossed with *yw*), *pepckΔ84*, and *pepckΔ84/Df(2R)ED3636* larvae. Results indicate that *pepckΔ84* allele is likely null or a strong hypomorph. Error bars indicate SD, $n = 3$. $^{**}P < 0.01$.

C PEPCK1 is dispensable for viability, but *pepckΔ84* homozygotes display lethality likely due to genetic background. Pupation and adult emergence of *pepckΔ84/+*, *pepckΔ84*, and *pepckΔ84/Df(2R)ED3636* animals.

D Loss of PEPCK1 leads to modest downregulation of circulating trehalose. Hemolymph was harvested from 3rd instar larvae grown on 20% yeast. Error bars indicate SD, $n = 10$. $^{**}P < 0.01$.

E Loss of PEPCK1 causes reduction of circulating glucose levels. Hemolymph was harvested from 3rd instar larvae grown on 20% yeast. Error bars indicate SD. $^{**}P < 0.01$.

F Loss of PEPCK1 strongly reduces circulating glycerol levels. Hemolymph was harvested from 3rd instar larvae grown on 20% yeast. Error bars indicate SD. $^{**}P < 0.01$.

G Triglyceride levels are reduced in the *pepck1* mutant male adult flies. Flies were aged for 5 days after eclosion on regular fly food. Errors bars indicate SD. $^{**}P < 0.01$.

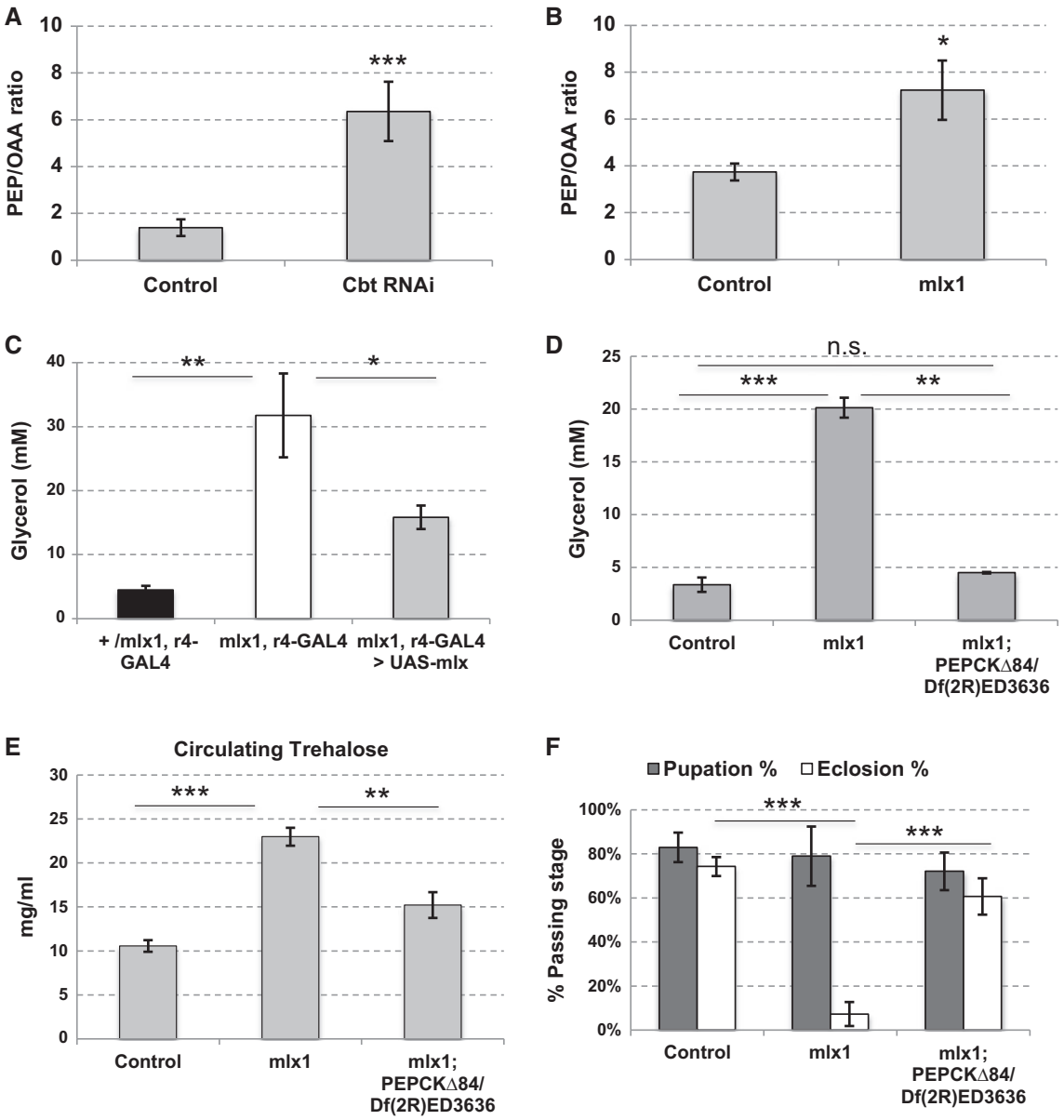


**Figure 5. The Mondo-Mlx/CBT transcriptional network controls PEPCK1-mediated cataplerosis.**

A, B cbtRNAi and *mlx*$^{1}$ mutant larvae display higher phosphoenolpyruvate (PEP) to oxaloacetate (OAA) ratio. Control (Tub-GAL80$^{ts}$; Tub-GAL4 > ), cbtRNAi (Tub-GAL80$^{ts}$; Tub-GAL4 > cbtRNAi NIG 4427R-1), control and *mlx*$^{1}$ mutants were grown on 20% yeast until 3$^{rd}$ instar. Error bars indicate SD, $n$ = 3 (A) or 4 (B). *$P < 0.05$, ***$P < 0.001$.

C *mlx*$^{1}$ mutants display highly elevated circulating glycerol levels that can partially be rescued by introduction of *mlx* expression in the fat body using r4-GAL4. +/*mlx*$^{1}$, r4-GAL4; *mlx*$^{1}$, r4-GAL4; and *mlx*$^{1}$, r4-GAL4 > UAS-mlx larvae were grown on 20% yeast. Hemolymph was harvested from 3$^{rd}$ instar larvae, and circulating levels of free glycerol were assayed. Error bars indicate SD, $n$ = 4. *$P < 0.05$, **$P < 0.01$.

D The elevated circulating glycerol phenotype of *mlx*$^{1}$ mutants is rescued by loss of *pepck1*. Control, *mlx*$^{1}$, and *mlx*$^{1}$; *pepckΔ84/Df(2R)ED3636* animals were grown on 20% yeast until 3$^{rd}$ larval instar; hemolymph was collected, and free glycerol was measured. Error bars indicate SD, $n$ = 3. **$P < 0.01$, ***$P < 0.001$.

E The elevated circulating trehalose of *mlx*$^{1}$ mutants is partially rescued by loss of *pepck1*. Control, *mlx*$^{1}$, and *mlx*$^{1}$; *pepckΔ84/Df(2R)ED3636* animals were grown on 20% yeast until 3$^{rd}$ larval instar; hemolymph was collected and subjected to trehalose measurement. Error bars indicate SD, $n$ = 4 (control and *mlx*$^{1}$) or 3 (*mlx*$^{1}$; *pepckΔ84/Df(2R)ED3636*). **$P < 0.01$, ***$P < 0.001$.

F *mlx*$^{1}$ mutant pupal lethality is rescued by loss of *pepck1*. Pupation and adult emergence of control, *mlx*$^{1}$, and *mlx*$^{1}$; *pepckΔ84/Df(2R)ED3636* animals grown on standard lab food. Error bars indicate SD, $n$ = 4. ***$P < 0.001$.

by simultaneous loss of *pepck1* (Fig 5D). We have earlier shown that the *mlx*$^{1}$ mutants display strongly elevated levels of circulating glucose and trehalose (Havula *et al*, 2013). Interestingly, we observed that the levels of circulating trehalose were normalized in the *mlx*$^{1}$; *pepckΔ84/Df(2R)ED3636* double mutants (Fig 5E), while in the case of circulating glucose, there was no significant rescue observed (Supplementary Fig S8B). *mlx*$^{1}$ mutant larvae display near complete pupal lethality (Havula *et al*, 2013). Strikingly, also this

 

phenotype was efficiently suppressed by the simultaneous loss of *pepck1* (Fig 5F). In sum, our data demonstrate that deregulation of *pepck1* expression leads to impaired metabolism in *mlx* mutant animals and contributes to the lethality of these animals.

#### CBT modulates the circadian transcriptional network

The data presented above demonstrated a role for CBT in metabolic gene regulation. Interestingly, *cbt* promoter region is bound by the circadian transcription factor CLK in a circadian fashion (Abruzzi *et al*, 2011). In addition, our gene expression profiling (see earlier chapter on CBT target genes) revealed that CBT targets display a significant overlap with CLK-regulated genes. Together, these suggest a role for CBT in integrating the circadian clock with metabolism. In order to determine the influence of CBT in the circadian system, we utilized the cbtOE flies, which would mimic a situation of high CBT activity in sugar-fed animals. Circadian rhythms in locomotor activity are the most studied behavioral output of the circadian system in *Drosophila*. Interestingly, CBT overexpression led to severe defects in circadian locomotor activity rhythms. While control flies were strongly rhythmic, most cbtOE flies (85.1%; Fig 6A) displayed no or very weak rhythms. Moreover, the small percentage of flies displaying circadian behavioral rhythms did so with very low power (Fig 6A). To determine whether these defects were associated with impaired oscillation of the core or output circadian-controlled genes, we generated RNA-seq libraries from control and cbtOE fly heads collected at 6 different times of the day. Despite the strong defects on circadian behavior, cbtOE flies displayed normal oscillations of the mRNA of core clock circadian components such as *tim, clk, vri,* and *per* (Fig 6B and data not shown). However, cbtOE flies had serious defects in clock-controlled output genes. While a small subset of genes displayed strong and significant oscillations in control and cbtOE strains, a large number of mRNA had altered oscillations in cbtOE flies (Fig 6B). Interestingly, we noticed that genes that oscillate only in control flies, but cease to oscillate in cbtOE flies, are strongly enriched for terms related to metabolism (Fig 6C). We also found a similar number of mRNAs that cycle only in cbtOE flies. This could be attributed to the fact that the overexpression of *cbt* is done using the *tim-gal4* driver, which displays strong oscillations in activity (our own unpublished observation), hence making a subset of CBT transcriptional targets to artificially oscillate in this strain.

The results described above demonstrate that CBT is sufficient for sculpting the transcriptional profile of circadian-regulated mRNAs related to metabolism. To explore the importance of endogenous CBT in circadian regulation, we performed a similar experiment in cbtRNAi flies. As in the cbtOE flies, downregulation of CBT did not significantly affect the oscillations of the circadian clock components (Fig 6D). A subset of mRNAs ceased to oscillate in cbtRNAi flies, suggesting that their oscillation is CBT dependent. Strikingly, we found a large subset of mRNAs, which cycles only in cbtRNAi flies (Fig 6D). This subset is highly enriched for metabolic genes (Fig 6E). In order to investigate this finding further, we compared the amplitude of oscillation of genes in both cbtRNAi and control flies. We found a small but statistically significant increase in the average amplitude of oscillating genes in cbtRNAi flies (Supplementary Fig S8C). In addition, we found that there are more cycling genes in the cbtRNAi flies and that this is true for all amplitude cutoffs (Fig 6F). These results demonstrate that CBT represses the oscillation of an important subset of metabolic genes regulated by the circadian clock.

## Discussion

In this study, we establish the *Drosophila klf10* ortholog, *cbt,* as a repressive effector of the sugar sensing transcriptional network. Specifically, we showed that: (i) *cbt* expression is activated by dietary sugars in *mlx*-dependent manner, (ii) *cbt* is a direct target of Mlx, (iii) many key metabolic genes are rapidly repressed by CBT upon sugar feeding, (iv) CBT binds to the proximity of *pepck* genes, (v) *pepck1* is dispensable for viability, but essential for glucose and glycerol homeostasis, (vi) deregulation of *pepck1* underlies lethality of *mlx* mutants, and (vii) CBT modulates the circadian system by controlling the cycling of a subset of circadian output genes. Based on these findings, we propose a model in which CBT serves as a repressive downstream effector of the Mondo-Mlx-mediated sugar sensing, which contributes to diet-induced physiological readjustment, including flux of central carbon metabolism and cycling of metabolic circadian clock targets.

By uncovering the CBT-mediated repression of *pepck* isoforms downstream of Mondo-Mlx, our study provides a mechanistic explanation to the regulation of cataplerosis in response to intracellular sugar sensing. *Drosophila* Mondo-Mlx is known to drive activation of glycolysis, for example, by promoting the expression of *phosphofructokinase 2* (Havula *et al*, 2013). Placing the rate-limiting enzymes of gluconeogenesis downstream, the same sensor mechanism that activates glycolysis provides an elegant mechanism to adjust the direction of flux of glucose metabolism in response

**Figure 6. Regulation of the circadian transcriptional network by *cbt*.**

A Circadian locomotor behavior of tim-cbtOE flies. Tim-cbtOE and their respective control adult flies were placed first for 3–4 days in 12:12 LD condition and then transferred into DD (constant darkness). Average actograms show their circadian activity during DD conditions. Rhythmic (RI $\geq$ 0.2) or arrhythmic activity pattern of these flies were grouped, and their average profiles were plotted. The percentage indicates the percentage of flies in each group (N = number of flies).

B Heatmap representation of genes cycling in both control and tim-cbtOE adult flies (upper panel), only in the control (middle), and only in RNAi flies (lower panel).

C Gene ontology (GO) enrichment analyses for cycling genes in either cbtOE or control adult flies. *P*-value < 0.05 after Bonferroni correction was used to determine statistical significance. NA indicates that the term did not reach statistical significance in this sample.

D Heatmap representation of genes cycling in both control and cbtRNAi adult flies (upper panel), only in the control (middle) and only in RNAi flies (lower panel).

E Gene ontology (GO) enrichment analyses results of cycling genes in cbtRNAi adult flies or in control. *P*-value < 0.05 after Bonferroni correction was used to determine statistical significance. NA indicates that the term did not reach statistical significance in this sample.

F More genes cycle in the RNAi adult flies compared to control. Selection of genes by different cutoff of the cycling amplitude (AMPL) shows similar patterns. Chi-square test demonstrated statistical significance of the differences (**$P$ < 0.001, *$P$ < 0.05).

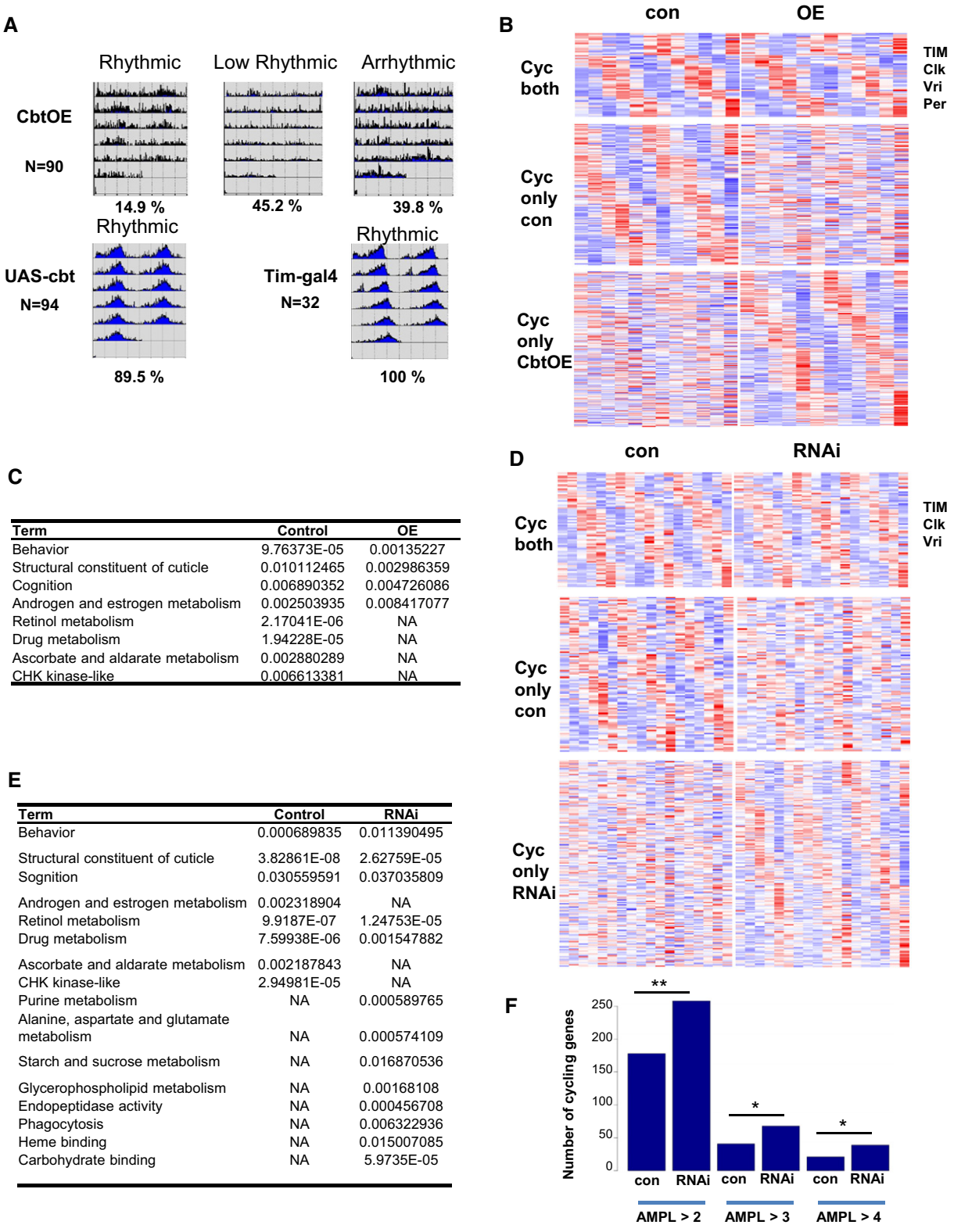


C

| Term | Control | OE |
|---|---|---|
| Behavior | 9.76373E-05 | 0.00135227 |
| Structural constituent of cuticle | 0.010112465 | 0.002986359 |
| Cognition | 0.006890352 | 0.004726086 |
| Androgen and estrogen metabolism | 0.002503935 | 0.008417077 |
| Retinol metabolism | 2.17041E-06 | NA |
| Drug metabolism | 1.94228E-05 | NA |
| Ascorbate and aldarate metabolism | 0.002880289 | NA |
| CHK kinase-like | 0.006613381 | NA |

E

| Term | Control | RNAi |
|---|---|---|
| Behavior | 0.000689835 | 0.011390495 |
| Structural constituent of cuticle | 3.82861E-08 | 2.62759E-05 |
| Sognition | 0.030559591 | 0.037035809 |
| Androgen and estrogen metabolism | 0.002318904 | NA |
| Retinol metabolism | 9.9187E-07 | 1.24753E-05 |
| Drug metabolism | 7.59938E-06 | 0.001547882 |
| Ascorbate and aldarate metabolism | 0.002187843 | NA |
| CHK kinase-like | 2.94981E-05 | NA |
| Purine metabolism | NA | 0.000589765 |
| Alanine, aspartate and glutamate metabolism | NA | 0.000574109 |
| Starch and sucrose metabolism | NA | 0.016870536 |
| Glycerophospholipid metabolism | NA | 0.00168108 |
| Endopeptidase activity | NA | 0.000456708 |
| Phagocytosis | NA | 0.006322936 |
| Heme binding | NA | 0.015007085 |
| Carbohydrate binding | NA | 5.9735E-05 |

**Figure 6.**

to sugar input. Such simple network topology provides a robust safeguard against loss of energy in futile cycles caused by simultaneous high activity of glycolysis and gluconeogenesis.

Mondo-Mlx also activates the expression of lipogenic gene expression (e.g., *FAS* and *ACC*) in order to promote conversion of excess sugars into triglycerides (Sassu *et al*, 2012; Havula *et al*,

2013). In addition to fatty acid moieties, which are built by FAS and ACC, triglyceride biosynthesis requires glycerol-3-phosphate. Substrate-labeling studies in mammals have shown that a significant portion of glycerol in triglycerides is in fact derived from the PEPCK-dependent glyceroneogenesis pathway (Kalhan *et al*, 2001; Chen *et al*, 2005; Nye *et al*, 2008; Jin *et al*, 2013). This is supported by our findings showing significantly lower circulating glycerol levels in well-fed *pepck1*-mutant larvae. The impact of glyceroneogenesis on triglyceride homeostasis is also likely reflected in the reduced triglyceride levels in *pepck1* mutant flies. Similarly, mammalian studies have shown that elevated expression of PEPCK-C in adipose tissue increases fat mass, whereas reduced PEPCK-C expression leads to lower fat content (Franckhauser *et al*, 2002; Olswang *et al*, 2002). Moreover, in humans, adipose tissue expression of PEPCK-C positively correlates with adiposity and plasma triacylglycerol levels (Chang *et al*, 2008). Control of *pepck* through CBT places both branches of triglyceride biosynthesis under Mondo-Mlx. Inhibition of PEPCK-mediated cataplerosis upon high sugar intake allows maximal conversion of excess glucose-6-phosphate into the glycerol moieties of triglycerides through the glycolytic route of glycerol-3-phosphate synthesis. Simultaneous impairment of *de novo* lipogenesis and failure to suppress glyceroneogenesis likely leads to the breakage of glycerol homeostasis and massive accumulation of circulating glycerol, as observed in *mlx* mutants. Interestingly, a recent study showed that fasting serum levels of glycerol predicted development of hyperglycemia and type 2 diabetes (Mahendran *et al*, 2013). It will be interesting to learn whether this diagnostic marker is associated with deregulation of *pepck* isoforms and the activity of ChREBP/MondoA-Mlx and Klf10-dependent transcriptional network.

According to the current view, Mondo/ChREBP and Mlx act mainly in nutrient sensing and metabolic regulation. In contrast, CBT and its human ortholog Klf10 are multifunctional transcription factors. In *Drosophila*, *cbt* was originally identified as a developmental regulator with an essential function in dorsal closure early in development (Muñoz-Descalzo *et al*, 2005). Moreover, *cbt* is a direct transcriptional target of the circadian transcription factor CLK (Kadener *et al*, 2007; Abruzzi *et al*, 2011), and we have established here that it is deeply involved in the control of the circadian transcriptional network. While CBT overexpression leads to strong behavioral abnormalities, they are not accompanied by noticeable changes in the oscillation of the core clock components in the fly heads. This suggests that it reflects a specific effect on circadian output. If the behavioral patterns were due to an effect in the general health of the animal, we would expect deregulation of core clock components. Despite the null effect of *cbt* overexpression in the expression of core clock genes, we observed that *cbt* modulates the expression of an important subset of CLK and circadian-controlled genes, most of which are involved in metabolic functions. We observed also strong effects of *cbt* downregulation in circadian oscillation of metabolic genes, establishing CBT as a new regulator of the circadian transcriptome. Interestingly, downregulation of CBT in circadian cells decreases the amplitude of oscillation of a large number of circadian-controlled genes, providing a direct link between food intake, circadian gene expression, and behavior. Given the established link between feeding time, metabolism, and the circadian system in *Drosophila* (Xu *et al*, 2008, 2011; Mattson *et al*, 2014), it will be interesting to further analyze the importance of CBT in this coordination.

Although the functional analysis in this study largely focused on the metabolic role of *pepck* regulation by Mondo-Mlx-CBT network, our microarray and RNA-seq analyses revealed other interesting CBT transcriptional targets including *bmm*. This gene is an ortholog of the human *adipocyte triglyceride lipase* gene, and it is an essential regulator of triglyceride stores in *Drosophila* (Grönke *et al*, 2005). *bmm* expression is positively regulated by the Forkhead transcription factor FoxO, which is activated during starvation through inhibition of insulin-like signaling (Wang *et al*, 2011). The sugar-dependent repression of *bmm* expression by CBT is in perfect agreement with the lipogenic role of Mondo-Mlx.

It has been proposed that CBT mammalian ortholog Klf10 acts as a negative feedback regulator for ChREBP-activated genes, including lipogenic genes *FAS* and *ACC* (Iizuka *et al*, 2011). This conclusion was based on suppression of ChREBP-activated transcription upon Klf10 overexpression in primary liver cells. We tested this model by analyzing the expression of Mondo-Mlx targets *FAS* and *ACC*, but observed no effect by cbtRNAi (Supplementary Fig S8D). In contrast, our genome-wide expression analysis of CBT loss-of-function flies revealed that the CBT-dependent branch of the sugar sensing transcriptional network mediates rapid repression of gene expression. It is interesting to note that while most metabolic targets of CBT are rapidly and persistently downregulated, *cbt* expression is rapidly attenuated during prolonged sugar feeding (see Supplementary Fig S1A). This is likely due to the negative autoregulation demonstrated earlier (Belacortu *et al*, 2012) and supported by our ChIP data. The finding that most of the identified CBT-dependent mRNAs are stably repressed for many hours after *cbt* levels have significantly attenuated suggests that CBT-mediated repression might involve regulation at the chromatin level. This is in agreement with the possible involvement of Sin3A in CBT-mediated repression (Spittau *et al*, 2007; Belacortu *et al*, 2012). Through such persistent regulatory marks, sugar feeding may have a long-lasting influence on metabolic homeostasis, which is a topic that certainly deserves to be more thoroughly analyzed in the future.

In sum, our work provides a mechanistic explanation for the transcriptional repression upon Mondo-Mlx-mediated intracellular sugar sensing through the transcription factor CBT. The CBT-mediated repressive branch of the sugar sensing network is involved in securing the mutually exclusive activity of glycolysis and gluconeogenesis and coordination of fatty acid and glycerol biosynthesis with respect to dietary sugar intake. Our study also establishes a mechanism for nutrient input into the circadian gene expression. As intracellular sugar sensing and circadian regulation are highly conserved processes, the insight achieved here in the genetically tractable *Drosophila* model should provide a new conceptual framework for forthcoming studies in human subjects and mammalian model systems.

## Materials and Methods

### Fly stocks and maintenance

Flies were reared at 25°C in 12 h light:12 h dark cycles on standard diets (detailed in Supplementary Methods). For defined nutrient studies, 1$^{st}$ instar larvae were collected from apple juice plates onto

food containing 20% (w/v) dry baker's yeast, 0.5% (w/v) agarose, 2.5% (v/v) Nipagin (methylparaben), and 0.7% propionic acid in PBS supplemented with or without 20% sucrose. For starvation, 2nd instar larvae were transferred to 0.5% agarose in PBS media for 16 h, followed by 4 h of refeeding with 0.5% agarose and 10% glucose in PBS media.

*Tim-gal4*, $cbt^{E1}$, *UAS-Dicer 2,* and UAS-cbt-Flag flies were previously described (Zhao *et al*, 2003; Muñoz-Descalzo *et al*, 2005; Dietzl *et al*, 2007). The P-element line P{EPgy2}EY10042 used to generate the *pepckΔ84* allele was from Bloomington Stock Center (19965). As a control for *pepckΔ84/Df(2R)ED3636,* we used a precise excision line in *trans* with *yw*. The RNAi lines used in this study were acquired from the following collections: RNAi lines targeting *cbt* from NIG-Fly Stock Center (4427R-1) and Vienna *Drosophila* RNAi Center (VDRC) (v15555); RNAi-line for *pepck1* (CG17725) v50253 from VDRC; and line 36915 for *pepck2* (CG10924) from Bloomington Stock Center. Control for $mlx^1$, $mlx^1$, UAS-mlx, and mondoRNAi (v109821) is detailed in Havula *et al* (2013).

#### Metabolite assays

Metabolite assays were performed using pre-wandering 3rd instar larvae grown on 20% yeast. Hemolymph was collected, and circulating glucose and trehalose were measured as described previously (Zhang *et al*, 2011). The circulating glycerol levels were determined by using the Free Glycerol Reagent (Sigma F6428) according to manufacturer's protocol, scaled down to 100 μl. Triglycerides from *pepck1* mutants were measured from 5-day-old adult male flies as described previously (Tennessen *et al*, 2014); values were normalized to protein. All measurements were done in minimum of three biological replicates. Student's *t*-test (two-tailed, unequal variance) was used for statistical analysis.

#### Sugar and protein feeding

For experimental manipulation, three-day-old Canton-S flies were starved for 16 h and then re-fed with agar-containing sucrose (5% sucrose) or protein (10% casein protein, Sigma). Flies were collected at time zero and at the indicated times after re-feeding.

#### Analysis of gene expression by real-time PCR

For analyses from fly heads, total RNA was prepared (30 heads per sample) using TRIzol reagent (Invitrogen) according to the manufacturer's protocol. cDNA derived from this RNA (using iScript, Bio-Rad) was utilized as a template for quantitative real-time PCR performed with the C1000 Thermal Cycler Bio-Rad. The PCR mixture contained Taq polymerase (SYBR green, Bio-Rad). Cycling parameters were 95°C for 3 min, followed by 40 cycles of 95°C for 10 s, 55°C for 10 s, and 72°C for 30 s. Fluorescence intensities were plotted versus the number of cycles by using an algorithm by the manufacturer. mRNA levels were quantified using a calibration curve based upon dilution of concentrated cDNA. mRNA values from heads were normalized to mRNAs encoding *ribosomal proteins 49* (*rp49*) and *RpS18*.

RNA from larvae was extracted using Nucleospin RNA XS or II kits (Macherey-Nagel). For quantitative RT–PCR, the RevertAid H Minus First Strand cDNA Synthesis Kit (Thermo Scientific) with random hexamer primers was used for first-strand cDNA synthesis. qPCR was performed using Maxima SYBR Green qPCR Master Mix (2×) (Thermo Fisher) and analyzed on Bio-Rad CFX384 Real-Time System with Bio-Rad CFX Manager. mRNA values from larvae were normalized to actin. Primer details are in Supplementary Methods.

#### Chromatin immunoprecipitation

Chromatin immunoprecipitation was performed from S2C cells (Mlx binding to *cbt* promoter) and from fly heads (Cabut targets). Experimental details are in Supplementary Methods.

#### Microarrays

RNA was used to prepare a probe that was hybridized to *Drosophila* 2.0 gene expression arrays (Affymetrix). CEL files were imported to Affymetrix Expression Console program, and data were normalized using Robust Multichips Analysis. Statistical analysis was performed using the R statistical environment (http://cran.r-project.org/). Differential expression was tested for all genes that had expression levels above 4.0 (log2 scale) for all measurements in at least one group (mutants or WT). To test for differential expression, we used analysis of variance (ANOVA), controlling for the effect of time of day. The *P*-values from the ANOVA were adjusted for multiple testing using the false discovery rate (FDR) correction implemented in the R-function p.adjust. We used two linear models with the genotype as the predictor. One model used genotype as the factor, and the second assumed gradual change between RNAi, control and overexpression. The *P*-values of both models were FDR corrected, and genes with $P < 0.2$ and at least 1.5 fold change between cbtRNAi and cbtOE were selected.

For enrichment analysis of cycling genes, we used previously published data of ~500 Clk target genes (Abruzzi *et al*, 2011) and crossed this list with the list of *cbt* upregulated or downregulated genes. Statistical significance was determined by comparing the results to multiple crossing of the Clk target genes with random set of genes (100,000 iterations).

#### RNA extraction, library preparation, and high-throughput sequencing

Fly heads of the indicated genotypes were collected, and RNA was extracted using TRI reagent (Sigma-Aldrich). RNA-seq libraries were prepared as previously described (Engreitz *et al*, 2013) with the modification of performing polyA selection after fragmentation. RNA-seq reads were aligned and counted per annotated gene.

##### *Analysis of control and cbtRNAi RNA-seq data*

We first filtered for expressed genes in each dataset separately (control or cbtRNAi). For each transcript, we determined whether it was differentially expressed in each sucrose concentration in comparison with the time zero control. To determine *P*-values, we utilized Dunett's method and performed an FDR correction. We chose those transcripts for which fold change > 1.5 and FDR < 0.4 in at least two different concentrations of sucrose. We determined

 

CBT dependence in the following cases: (i) genes that fit the significance criteria in control but not in the cbtRNAi dataset; (ii) those genes significantly upregulated in cbtRNAi flies but not in control flies; and (iii) genes that are more than 1.5-fold less affected in cbtRNAi while comparing to control.

*Time course RNA-seq profile*

We performed ANOVA and FDR correction in order to identify transcripts differentially expressed at any time point following sugar intake. From this group, we selected genes with more than 1.5-fold change. To avoid genes that showed significant changes due to circadian control, we eliminated those genes for which the difference between the first (0 h) and last (18 h) time points was less than 1.5-fold. We followed by clustering the differentially expressed into ten modules using hclust clustering, R bioconductor package. The clustering was based on Euclidean distance measured and clustered using the complete linkage method.

*Analysis of cycling genes*

The R package JTK cycle was used to detect cycling transcripts as described before (Hughes *et al*, 2010). We considered cycling transcript as transcript with $P$-value < 0.01 in the JTK analysis and an amplitude (minimum/maximum value) higher than 2 in all replicas. Chi-square tests were used to determine statistical significance of the differences in the number of cycling genes in the control versus RNAi files. Mann–Whitney $U$-test was used to determine statistical significance of difference in amplitude size between cycling genes in cbtRNAi and control flies.

Heatmaps were generated using the heatmap.2 function of the gplots package in R. For each heatmap, we used k-means clustering for initial clustering of 6 groups, and a second hierarchical clustering for clustering genes within each group. DAVID functional annotation tool (http://david.abcc.ncifcrf.gov/home.jsp) (Huang *et al*, 2009) was used to examine gene ontology (GO) enrichment in the different gene groups. $P$-value < 0.05 after Bonferroni correction was used to determine statistical significance.

#### Circadian locomotor behavior

Adult male and female flies (3–7 days old) were used for circadian locomotor behavior; these flies were placed separately in behavioral glass tubes containing sucrose–agar food (2% agar, BD; 5% sucrose, BioLab). First, flies were entrained in LD (light:dark) condition for the first 3–4 days, followed by 7–11 days in DD (constant dark); activity was monitored by using Trikinetics Drosophila Activity Monitors (DAM; Trikinetics, Waltham, MA) system. Data were collected by DAM System 3 Data collection software and analyzed using MatLab, as described before (Levine *et al*, 2002). Rhythm index of > 0.2 in DD was used as threshold for defining activity as rhythmic. Constant humidity and temperature (25 ± 1°C) were maintained during the experiment.

#### Phosphoenolpyruvate/oxaloacetate ratio measurement

Phosphoenolpyruvate (PEP), pyruvate, and oxaloacetate (OAA) concentrations were measured fluorometrically according to the kits' manufacturer's guidelines (MAK102, MAK070, Sigma-Aldrich); the assay is detailed in Supplementary Methods.

#### Data deposition

Our functional genomics data were deposited into Gene Expression Omnibus (GEO) under accession codes GSE58854, GSE67865 and GSE67590.

**Supplementary information** for this article is available online: http://emboj.embopress.org


### Acknowledgements

We thank Heini Seppälä and Yuval Weighl for technical assistance and our lab members for feedback. Guillaume Huet is thanked for the help with ChIP and N. Paricio for providing the anti-CBT antibody. We also thank Michael Rosbash for helpful discussions and support of Anand Vodola at Brandeis. MT was supported by the GBPM and ILS graduate programs. MP was supported by the Academy of Finland (#133223). SK was supported by the European Research Council Starting Grant (ERC #260911) and the Israeli Science Foundation Personal Grant (ISF #840/14). VH was supported by ERC Starting Grant (#281720), Academy of Finland (#129964), Sigrid Juselius Foundation, Novo Nordisk Foundation and Biocentrum Helsinki.


### Conflict of interest

The authors declare that they have no conflict of interest.

### Author contributions

OB, MT, VP, YN, SK, and VH designed experiments. OB, MT, VP, MH, BMR, EH, AM, and SV performed experiments. MT, RA, MH, SK, and VH analyzed data. BMR and MP provided reagents or analysis tools. OB, MT, RA, SK, and VH wrote the manuscript.

## References


Abruzzi KC, Rodriguez J, Menet JS, Desrochers J, Zadina A, Luo W, Tkachev S, Rosbash M (2011) Drosophila CLOCK target gene characterization: implications for circadian tissue-specific gene expression. *Genes Dev* 25: 2374 – 2386

Ballard FJ, Hanson RW, Leveille GA (1967) Phosphoenolpyruvate carboxykinase and the synthesis of glyceride-glycerol from pyruvate in adipose tissue. *J Biol Chem* 242: 2746 – 2750

Bass J (2012) Circadian topology of metabolism. *Nature* 491: 348 – 356

Becker A, Schlöder P, Steele JE, Wegener G (1996) The regulation of trehalose metabolism in insects. *Experientia* 52: 433 – 439

Belacortu Y, Weiss R, Kadener S, Paricio N (2012) Transcriptional activity and nuclear localization of Cabut, the Drosophila ortholog of vertebrate TGF-β-inducible early-response gene (TIEG) proteins. *PLoS ONE* 7: e32004

Benhamed F, Denechaud PD, Lemoine M, Robichon C, Moldes M, Bertrand-Michel J, Ratziu V, Serfaty L, Housset C, Capeau J, Girard J, Guillou H, Postic C (2012) The lipogenic transcription factor ChREBP dissociates hepatic steatosis from insulin resistance in mice and humans. *J Clin Invest* 122: 2176 – 2194

Brown JL, Grau DJ, DeVido SK, Kassis JA (2005) An Sp1/KLF binding site is important for the activity of a Polycomb group response element from the Drosophila engrailed gene. *Nucleic Acids Res* 33: 5181 – 5189

Chang TJ, Lee WJ, Chang HM, Lee KC, Chuang LM (2008) Expression of subcutaneous adipose tissue phosphoenolpyruvate carboxykinase correlates with body mass index in nondiabetic women. *Metabolism* 57: 367 – 372

Chen JL, Peacock E, Samady W, Turner SM, Neese RA, Hellerstein MK, Murphy EJ (2005) Physiologic and pharmacologic factors influencing glyceroneogenic contribution to triacylglyceride glycerol measured by mass isotopomer distribution analysis. *J Biol Chem* 280: 25396 – 25402

Dibner C, Schibler U (2015). Circadian timing of metabolism in animal models and humans. *J Intern Med* 277: 513 – 527

Dietzl G, Chen D, Schnorrer F, Su KC, Barinova Y, Fellner M, Gasser B, Kinsey K, Oppel S, Scheiblauer S, Couto A, Marra V, Keleman K, Dickson BJ (2007) A genome-wide transgenic RNAi library for conditional gene inactivation in Drosophila. *Nature* 448: 151 – 156

Eissing L, Scherer T, Tödter K, Knippschild U, Greve JW, Buurman WA, Pinnschmidt HO, Rensen SS, Wolf AM, Bartelt A, Heeren J, Buettner C, Scheja L (2013) De novo lipogenesis in human fat and liver is linked to ChREBP-β and metabolic health. *Nat Commun* 4: 1528

Engreitz JM, Pandya-Jones A, McDonel P, Shishkin A, Sirokman K, Surka C, Kadri S, Xing J, Goren A, Lander ES, Plath K, Guttman M (2013) The Xist lncRNA exploits three-dimensional genome architecture to spread across the X chromosome. *Science* 341: 1237973

Filhoulaud G, Guilmeau S, Dentin R, Girard J, Postic C (2013) Novel insights into ChREBP regulation and function. *Trends Endocrinol Metab* 24: 257 – 268

Franckhauser S, Muñoz S, Pujol A, Casellas A, Riu E, Otaegui P, Su B, Bosch F (2002) Increased fatty acid re-esterification by PEPCK overexpression in adipose tissue leads to obesity without insulin resistance. *Diabetes* 51: 624 – 630

Grönke S, Mildner A, Fellert S, Tennagels N, Petry S, Müller G, Jäckle H, Kühnlein RP (2005) Brummer lipase is an evolutionary conserved fat storage regulator in Drosophila. *Cell Metab* 1: 323 – 330

Guillaumond F, Gréchez-Cassiau A, Subramaniam M, Brangolo S, Peteri-Brünback B, Staels B, Fiévet C, Spelsberg TC, Delaunay F, Teboul M (2010) Kruppel-like factor KLF10 is a link between the circadian clock and metabolism in liver. *Mol Cell Biol* 30: 3059 – 3070

Gutierrez-Aguilar R, Benmezroua Y, Balkau B, Marre M, Helbecque N, Charpentier G, Polychronakos C, Sladek R, Froguel P, Neve B (2007) Minor contribution of SMAD7 and KLF10 variants to genetic susceptibility of type 2 diabetes. *Diabetes Metab* 33: 372 – 378

Hanson RW, Reshef L (2003) Glyceroneogenesis revisited. *Biochimie* 85: 1199 – 1205

Hardin PE (2011) Molecular genetic analysis of circadian timekeeping in Drosophila. *Adv Genet* 74: 141 – 173

Havula E, Hietakangas V (2012) Glucose sensing by ChREBP/MondoA-Mlx transcription factors. *Semin Cell Dev Biol* 23: 640 – 647

Havula E, Teesalu M, Hyötyläinen T, Seppälä H, Hasygar K, Auvinen P, Orešič M, Sandmann T, Hietakangas V (2013) Mondo/ChREBP-Mlx-regulated transcriptional network is essential for dietary sugar tolerance in Drosophila. *PLoS Genet* 9: e1003438

Hietakangas V, Cohen SM (2009) Regulation of tissue growth through nutrient sensing. *Annu Rev Genet* 43: 389 – 410

Huang DW, Sherman BT, Lempicki RA (2009) Systematic and integrative analysis of large gene lists using DAVID bioinformatics resources. *Nat Protoc* 4: 44 – 57

Hughes ME, Hogenesch JB, Kornacker K (2010) JTK_CYCLE: an efficient nonparametric algorithm for detecting rhythmic components in genome-scale data sets. *J Biol Rhythms* 25: 372 – 380

Iizuka K, Takeda J, Horikawa Y (2011) Krüppel-like factor-10 is directly regulated by carbohydrate response element-binding protein in rat primary hepatocytes. *Biochem Biophys Res Commun* 412: 638 – 643

Ishii S, Iizuka K, Miller BC, Uyeda K (2004) Carbohydrate response element binding protein directly promotes lipogenic enzyme gene transcription. *Proc Natl Acad Sci USA* 101: 15597 – 15602

Jeong YS, Kim D, Lee YS, Kim HJ, Han JY, Im SS, Chong HK, Kwon JK, Cho YH, Kim WK, Osborne TF, Horton JD, Jun HS, Ahn YH, Ahn SM, Cha JY (2011) Integrated expression profiling and genome-wide analysis of ChREBP targets reveals the dual role for ChREBP in glucose-regulated gene expression. *PLoS ONE* 6: e22544

Jin ES, Sherry AD, Malloy CR (2013) Metabolism of glycerol, glucose, and lactate in the citric acid cycle prior to incorporation into hepatic acylglycerols. *J Biol Chem* 288: 14488 – 14496

Kadener S, Stoleru D, McDonald M, Nawathean P, Rosbash M (2007) Clockwork Orange is a transcriptional repressor and a new Drosophila circadian pacemaker component. *Genes Dev* 21: 1675 – 1686

Kalhan SC, Mahajan S, Burkett E, Reshef L, Hanson RW (2001) Glyceroneogenesis and the source of glycerol for hepatic triacylglycerol synthesis in humans. *J Biol Chem* 276: 12928 – 12931

Kooner JS, Chambers JC, Aguilar-Salinas CA, Hinds DA, Hyde CL, Warnes GR, Gómez Pérez FJ, Frazer KA, Elliott P, Scott J, Milos PM, Cox D, Thompson JF (2008) Genome-wide scan identifies variation in MLXIPL associated with plasma triglycerides. *Nat Genet* 40: 149 – 151

Levine JD, Funes P, Dowse HB, Hall JC (2002) Signal analysis of behavioral and molecular cycles. *BMC Neurosci* 3: 1

Mahendran Y, Cederberg H, Vangipurapu J, Kangas AJ, Soininen P, Kuusisto J, Uusitupa M, Ala-Korpela M, Laakso M (2013) Glycerol and fatty acids in serum predict the development of hyperglycemia and type 2 diabetes in Finnish men. *Diabetes Care* 36: 3732 – 3738

Masri S, Sassone-Corsi P (2014). Sirtuins and the circadian clock: bridging chromatin and metabolism. *Sci Signal* 7, re6

Mattson MP, Allison DB, Fontana L, Harvie M, Longo VD, Malaisse WJ, Mosley M, Notterpek L, Ravussin E, Scheer FAJL, Seyfried TN, Varady KA, Panda S (2014) Meal frequency and timing in health and disease. *Proc Natl Acad Sci USA* 111: 16647 – 16653

Muñoz-Descalzo S, Terol J, Paricio N (2005) Cabut, a C2H2 zinc finger transcription factor, is required during Drosophila dorsal closure downstream of JNK signaling. *Dev Biol* 287: 168 – 179

Nye CK, Hanson RW, Kalhan SC (2008) Glyceroneogenesis is the dominant pathway for triglyceride glycerol synthesis in vivo in the rat. *J Biol Chem* 283: 27565 – 27574

Oh KJ, Han HS, Kim MJ, Koo SH (2013) CREB and FoxO1: two transcription factors for the regulation of hepatic gluconeogenesis. *BMB Rep* 46: 567 – 574

Olswang Y, Cohen H, Papo O, Cassuto H, Croniger CM, Hakimi P, Tilghman SM, Hanson RW, Reshef L (2002) A mutation in the peroxisome proliferator-activated receptor gamma-binding site in the gene for the cytosolic form of phosphoenolpyruvate carboxykinase reduces adipose tissue size and fat content in mice. *Proc Natl Acad Sci USA* 99: 625 – 630

Partch CL, Green CB, Takahashi JS (2014) Molecular architecture of the mammalian circadian clock. *Trends Cell Biol* 24: 90 – 99

Peek CB, Ramsey KM, Marcheva B, Bass J (2012) Nutrient sensing and the circadian clock. *Trends Endocrinol Metab* 23: 312 – 318

Qi Q, Chu AY, Kang JH, Jensen MK, Curhan GC, Pasquale LR, Ridker PM, Hunter DJ, Willett WC, Rimm EB, Chasman DI, Hu FB, Qi L (2012) Sugar-sweetened beverages and genetic risk of obesity. *N Engl J Med* 367: 1387 – 1396

Sassu ED, McDermott JE, Keys BJ, Esmaeili M, Keene AC, Birnbaum MJ, DiAngelo JR (2012) Mio/dChREBP coordinately increases fat mass by

 

regulating lipid synthesis and feeding behavior in Drosophila. *Biochem Biophys Res Commun* 426: 43 – 48

Spittau B, Krieglstein K (2012) Klf10 and Klf11 as mediators of TGF-beta superfamily signaling. *Cell Tissue Res* 347: 65 – 72

Spittau B, Wang Z, Boinska D, Krieglstein K (2007) Functional domains of the TGF-beta-inducible transcription factor Tieg3 and detection of two putative nuclear localization signals within the zinc finger DNA-binding domain. *J Cell Biochem* 101: 712 – 722

Stanhope KL, Schwarz JM, Havel PJ (2013) Adverse metabolic effects of dietary fructose: results from the recent epidemiological, clinical, and mechanistic studies. *Curr Opin Lipidol* 24: 198 – 206

Stark R, Guebre-Egziabher F, Zhao X, Feriod C, Dong J, Alves TC, Ioja S, Pongratz RL, Bhanot S, Roden M, Cline GW, Shulman GI, Kibbey RG (2014) A role for mitochondrial phosphoenolpyruvate carboxykinase (PEPCK-M) in the regulation of hepatic gluconeogenesis. *J Biol Chem* 289: 7257 – 7263

Subramaniam M, Hawse JR, Bruinsma ES, Grygo SB, Cicek M, Oursler MJ, Spelsberg TC (2010) TGFbeta inducible early gene-1 directly binds to, and represses, the OPG promoter in osteoblasts. *Biochem Biophys Res Commun* 392: 72 – 76

Tennessen JM, Barry WE, Cox J, Thummel CS (2014). Methods for studying metabolism in Drosophila. *Methods San Diego Calif* 68: 105 – 115

Wang B, Moya N, Niessen S, Hoover H, Mihaylova MM, Shaw RJ, Yates JR 3rd, Fischer WH, Thomas JB, Montminy M (2011) A hormone-dependent module regulating energy balance. *Cell* 145: 596 – 606

Weiss R, Bartok O, Mezan S, Malka Y, Kadener S (2014) Synergistic interactions between the molecular and neuronal circadian networks drive robust behavioral circadian rhythms in Drosophila melanogaster. *PLoS Genet* 10: e1004252

Xu K, DiAngelo JR, Hughes ME, Hogenesch JB, Sehgal A (2011) The circadian clock interacts with metabolic physiology to influence reproductive fitness. *Cell Metab* 13: 639 – 654

Xu K, Zheng X, Sehgal A (2008) Regulation of feeding and metabolism by neuronal and peripheral clocks in Drosophila. *Cell Metab* 8: 289 – 300

Zhang H, Chen Q, Yang M, Zhu B, Cui Y, Xue Y, Gong N, Cui A, Wang M, Shen L, Zhang S, Fang F, Chang Y (2013) Mouse KLF11 regulates hepatic lipid metabolism. *J Hepatol* 58: 763 – 770

Zhang W, Thompson BJ, Hietakangas V, Cohen SM (2011) MAPK/ERK signaling regulates insulin sensitivity to control glucose metabolism in Drosophila. *PLoS Genet* 7: e1002429

Zhao J, Kilman VL, Keegan KP, Peng Y, Emery P, Rosbash M, Allada R (2003) Drosophila clock can generate ectopic circadian clocks. *Cell* 113: 755 – 766